A Theory for the Rate Constant of a Dissociative Proton-Coupled Electron-Transfer Reaction

R. I. Cukier

Department of Chemistry, Michigan State University, East Lansing, Michigan 48824-1322

Received: January 27, 1999; In Final Form: May 21, 1999

A theory that predicts the rate of a dissociative proton-coupled electron-transfer reaction is presented. The electron and proton transfer is treated as one quantum event that is driven by the coupling of the respective charges to the solvent's orientational polarization. The final state, where both electron and proton have transferred, corresponds to a repulsive surface for the proton motion. Consequently, the reaction products include a dissociated proton-transferred species. The origin of the repulsive surface is attributed to a combination of the hydrogen bond's relative weakness and the role of the solvent's electronic polarization in aiding the dissociation. The rate constant depends on the reaction free energy and reorganization energy, the bound state energies and wave functions in the initial proton surface, and the parameters of the proton final state repulsive surface. The rate constant can be quite large and should provide a reaction pathway competitive with consecutive electron and proton transfer.

I. Introduction

Coupled electron and proton transfer is a reaction pathway of some generality that has stimulated experimental[1−17] and theoretical studies.[18−28] Often, it is difficult to decide whether the process is consecutive—electron transfer followed by proton transfer (ET/PT) or vice versa (PT/ET)—or a concerted process, where the two species transfer together in one quantum mechanical tunneling event. When the electron and proton are associated with the same atom, the coupled transfer can be considered as a hydrogen atom transfer, complicating the distinction between concerted and consecutive mechanisms. In this work, we will focus on concerted electron−proton transfer (ETPT) where the acceptors for the electron and proton are different species, thus precluding hydrogen atom transfer. Furthermore, we shall consider reactions where the final state is dissociative and denote the process as DETPT. As a *consecutive* process, the reaction may be schematized as

$$A + R_1OH\cdots NR_2 \xrightarrow{ET} A^- + [R_1OH\cdots NR_2]^{\bullet +} \xrightarrow{PT}$$
$$A^- + [R_1O\cdots HNR_2]^{\bullet +} \xrightarrow{diss} A^- + [R_1O]^{\bullet} + [HNR_2]^+$$

As a *concerted* process, the reaction is

Scheme 1

$$A + R_1OH\cdots NR_2 \xrightarrow{DETPT} A^- + [R_1O]^{\bullet} + [HNR_2]^+$$

The concerted process involves the simultaneous transfer of an electron and proton, with the proton final state characterized by a repulsive potential energy surface (pes).

There is ample evidence of reactions that lead to the overall conversion to yield the product species as shown in Scheme 1, though it is not easy to prove that the process is consecutive. In the realm of biology, a step in the chain of charge transfers in the photosystem II oxygen evolving complex (PSII/OEC) may provide an example of DETPT.[4,29−33] There is a reaction center chlorophyll P680 that has been previously oxidized to $P680^+$. A tyrosine labeled conventionally as Y_Z is hydrogen bonded to a nearby histidine residue. This tryrosine is oxidized to a tryrosyl radical and re-reduces $P680^+$ to P680. The proton in the tyrosyl−histidine hydrogen bond transfers from the phenol to the nitrogen of the base, and there is no evidence for a hydrogen bonded proton at a well-defined distance. Thus, the postulation of a dissociative step is introduced. An extensive study by Linschitz and co-workers[34,35] of the quenching of triplet C_{60} by phenols in the presence of substituted pyridines does provide unambiguous evidence for concerted DETPT. The phenoxy radical and the protonated base are the observed reaction products, in addition to $C_{60}^{\bullet -}$, demonstrating the concerted nature of this DETPT reaction. As another example, radiation-induced electron-transfer reactions of substituted phenols in low-temperature glasses show the production of the phenol radical cation that disappears upon warming.[36] But, also seen within the time scale of the initiating pulse is formation of *phenoxy* radicals, indicating a dissociative pathway. And, in polar solvents, the immediate, exclusive reaction product is the phenoxy radical. Thus, this is an example where both consecutive and concerted reaction pathways are present with the ultimate products corresponding to DETPT.

In previous work on ETPT we have stressed that an enhanced pK_a of the hydrogen-bonded complex upon electron transfer favors the concerted mechanism.[23] If the proton surface after ET is sufficiently "tipped" to a downhill direction, then what was a double well proton potential may now have just a single minimum corresponding to the proton having transferred. Such a situation is favored by strong hydrogen bonds or, equivalently, by small flanking group distances.[37] In this regard, recent ab initio studies of phenol water[38] and phenol N_2[39] hydrogen-bonded complexes have shown that the radical cation complexes have flanking group distances that are significantly shorter than the corresponding neutral complexes. This suggests the possibility of vanishing or small barriers for the cation's proton-transfer surface. Furthermore, when additional waters are added to the cation radical complex the proton-transferred forms become the stable species.[40] For the cation radical of phenol

10.1021/jp990329a CCC: $18.00
Published on Web 07/09/1999

hydrogen bonded to ammonia, Bertran and co-workers found that only the proton-transferred species was stable,[41] a conclusion also reached by Yi and Scheiner.[42] They also found that increasing the number of coordinated ammonia molecules makes the proton-transferred species more stable.[42] These works show that after ET, when a cation is formed, there is a strong tendency for the proton to transfer too. Of course, this does not necessarily imply that the proton-transferred species will dissociate. Once the proton has transferred, dissociation is governed by the relatively weak, but still bound, $[R_1O\cdots HNR_2]^{\bullet+}$ hydrogen bond. With regard to the fast degrees of freedom (with respect to the transferring charge), the appropriate surface for discussing proton transfer (and also ETPT) is the *electronically* solvated proton pes, which we have referred to as a *pels* surface.[43] The solvent's electronic polarization is fast relative to the proton motion, and the relevant surface is actually an electronic degrees of freedom solvated potential of mean force. This solvation, when added to the gas-phase hydrogen-bonded surface, can be sufficient to produce a repulsive surface. Thus, in view of the experimental evidence, and the calculations presented below, there is reason to assert that the proton-transferred species can dissociate on the basis of a repulsive pes. As such, it is worth extending our previous ETPT theory to this dissociative case.

In addition to the pels surface, the slow nuclear degrees of freedom (the solvent's orientational polarization in dielectric continuum language[44,45]), also must be accounted for in a charge-transfer theory. For ETPT, we previously provided two approaches to the calculation of a rate constant, termed the double-adiabatic (DA) and the two-dimensional (2D) approaches.[20−24] In the DA theory,[22] ET is coupled to two modes—the solvent polarization (treated classically) and the proton displacement in the hydrogen bond interface. For ETPT, the proton does not undergo a small displacement. Rather, it actually does transfer. In the 2D approach, the electron and proton are both considered as quantum objects in a two-dimensional tunneling space, with one tunnel coordinate for the electron and one for the proton. That both electron and proton are tunneling in one quantum event is conceptually clear in this approach. The condition that tunneling can take place is the equality of initial and final energies of interaction of the electron and proton with the solvent. These energies are parametric on the solvent nuclear configuration, as in conventional ET theory.[44,45] We are therefore making the same separation between the fast electronic solvent polarization (to construct the pels surfaces), the intermediate speed transferring charges (electron and proton), and the slow orientational polarization of the solvent that is made in the Marcus formulation of electron-transfer theory.[44,45]

Due to the mass disparity between the proton and electron, the 2D tunnel path may be approximated as a "zigzag" path where the proton displaces adiabatically along its coordinate to a certain configuration that permits the electron to tunnel (one-dimensionally) along its coordinate.[22] Then, the proton, with the electron now in its final state, relaxes to its final state. This restricted tunnel path leads to a rate constant expression involving an electronic matrix element that connects the electron in its initial and final states and a series of Franck−Condon factors for the proton before and after transfer. The resulting expression is the same as that obtained by using the DA approach, but the method of derivation clarifies the nature of ETPT.

The DA approach provides a convenient starting point for a DETPT theory. The principle modification is the treatment of the Franck−Condon (FC) factors for the overlap of the proton initial and final eigenstates, when the final proton state is characterized by a repulsive pes. Then the sum over final proton states becomes an integration over a continuum of states, and bound−unbound FC factors need to be evaluated. The issues are similar to those that arise in electron-transfer reactions that involve bond-breaking.[46−48] Recent work by German and Kuznetsov[48] suggest several approaches to the evaluation of the bound−unbound FC factors in the context of bond-breaking electron-transfer reactions. If the motion along the repulsive surface for the dissociation can be treated classically, then simplified expressions can be generated for the rate constant. We will follow a similar strategy here.

The plan of the remainder of this paper follows. In section II the rate constant for DETPT is formulated and manipulated into an expression suitable for numerical evaluation. Section III constructs the electronically solvated potential energy surface that can account for proton dissociation. The rate constant is numerically evaluated, and its dependence on the relevant parameters is explored, in section IV. Our conclusions are summarized in section V.

II. Rate Constant Formulation

To evaluate the rate constant describing the concerted charge transfer, it is convenient to work in a basis of localized initial and final electron/proton states that we denote respectively as 1 and 2. All the terms in the Hamiltonian describing the solute and solvent are diagonal in the localized basis except for the term proportional to the electronic coupling V_{el} that is responsible for the transfer. If V_{el} is sufficiently small, then the transition rate between states 1 and 2 is given by the Golden rule expression[22,49]

$$k = \frac{V_{el}^2}{\hbar^2}\sum_{j'}\sum_{n'}P_{1j'}\rho_{1n'}\sum_{j}\sum_{n}|\langle\Pi_{2j}|\Pi_{1j'}\rangle|^2|\langle\chi_{2n}|\chi_{1n'}\rangle|^2 \times \delta(E_{1j'} - E_{2j} + \epsilon_{1n'} - \epsilon_{2n}) \quad (2.1)$$

The energies $E_{ij}(\epsilon_{in})$, vibronic wave functions Π_{ij} (χ_{in}) $(i = 1, 2)$, and Boltzmann factors $P_{1j} = e^{-E_{1j'}/k_BT}/Q_s(\rho_{1n'} = e^{-\epsilon_{1n}'/k_BT}/Q)$ are those of the solvent polarization (proton mode), and the squares of the terms in $|\ |$ are the corresponding Franck−Condon factors. As we shall treat the solvent polarization classically and the proton initial state mode quantum mechanically, it is convenient to write the energy conservation δ function in the form[50]

$$\delta(E_{1j'} - E_{2j} + \epsilon_{1n'} - \epsilon_{2n}) = \int d\epsilon\ \delta(E_{1j'} - E_{2j} - \epsilon)\ \delta(\epsilon + \epsilon_{1n'} - \epsilon_{2n}) \quad (2.2)$$

The use of eq 2.2 in eq 2.1 permits separation of the sums over the two modes as

$$k = \frac{V_{el}^2}{\hbar^2}\int d\epsilon \sum_{n'}\rho_{1n'}\sum_{n}|\langle\chi_{2n}|\chi_{1n'}\rangle|^2\ \delta(\epsilon_{1n'} - \epsilon_{2n} + \epsilon) \int_{-\infty}^{+\infty} dt\ e^{i(\epsilon+\Delta G^\circ)t/\hbar}\langle e^{itH_2/\hbar}\ e^{-itH_1/\hbar}\rangle \quad (2.3)$$

The solvent orientational polarization mode has been reexpressed by writing its energy δ function as a Fourier time integral and introducing the Hamiltonians H_1 (H_2) corresponding to the polarization for the initial (final) electron/proton states.[51] The reaction free energy difference is denoted as ΔG°. In the classical limit, the polarization contribution is[49]

$$\int_{-\infty}^{+\infty} dt\, e^{i(\epsilon+\Delta G^\circ)t/\hbar}\langle e^{itH_2/\hbar}\, e^{-itH_1/\hbar}\rangle = [\hbar^2/\lambda_s k_B T]^{1/2} \exp[-(\epsilon+\lambda_s+\Delta G^\circ)^2/4\lambda_s k_B T] \quad (2.4)$$

where the solvent reorganization energy is denoted as λ_s. Introducing a time Fourier representation of the $\delta(\epsilon_{1n'} - \epsilon_{2n} + \epsilon)$ function lets us express eq 2.3 in the form

$$k = \frac{1}{2\pi\hbar}\frac{V_{el}^2}{[\lambda_s k_B T]}\frac{1}{Q}\int d\epsilon \int_{-\infty}^{+\infty}\frac{dt}{\hbar}\int dq \int dq'\, \rho_1(q,q'|\beta - it)\, \rho_2(q,q'|it) \exp[-(\lambda_s+\Delta G^\circ+\epsilon)^2/4\lambda_s k_B T] \quad (2.5)$$

where the coordinate (q) space density matrices for the proton, of the indicated complex temperatures ($\beta = 1/k_B T$), are defined as

$$\rho_1(q,q'|\beta - it) = \sum_{n'}\chi_{1n'}(q)\,\chi_{1n'}(q)\, e^{-(\beta - it/\hbar)\epsilon_{1n'}}$$

$$\rho_2(q,q'|it) = \sum_{n}\chi_{2n}(q)\,\chi_{2n}(q')\, e^{-(it/\hbar)\epsilon_{1n}} \quad (2.6)$$

The Gaussian integration over the energy variable ϵ is readily carried out to yield

$$k = \frac{V_{el}^2}{\pi^{1/2}\hbar}\frac{1}{Q}\int_{-\infty}^{+\infty}\frac{dt}{\hbar}\int dq \int dq'\, \rho_1(q,q'|\beta - it)\, \rho_2(q,q'|it)\, e^{-it(\lambda_s+\Delta G^\circ)/\hbar} e^{-(t^2/\hbar^2)\lambda_s k_B T} \quad (2.7)$$

This expression is convenient for introducing the classical approximation to the final state surface as

$$\rho_2(q,q'|it) = e^{-(it/\hbar)V_2(q)}\,\delta(q-q') \quad (2.8)$$

The use of this classical approximation in eq 2.7, with reexpression of the ρ_2 density matrix in terms of the wave functions of eq 2.6, and another Gaussian integration, produces our working result:

$$k = \frac{V_{el}^2}{\hbar[\lambda_s k_B T]^{1/2}}\sum_{n'=0}\rho_{1n'}\int dq\, |\chi_{1n'}(q)|^2 \exp[-(\lambda_s+\Delta G^\circ+V_2(q)-\epsilon_{1n'})^2/4\lambda_s k_B T] \quad (2.9)$$

If only the ground vibrational state in the initial proton pes were to contribute to the rate, eq 2.9 would reduce to

$$k = \frac{V_{el}^2}{\hbar[\lambda_s k_B T]^{1/2}}\int dq\, \frac{\rho_1(q,q)}{Q} \exp[-(\lambda_s+\Delta G^\circ+V_2(q)-\epsilon_{10})^2/4\lambda_s k_B T] \quad (2.10)$$

This rate constant may be viewed as an effective activation energy that is q-dependent (the exponential term), averaged over the probability density of the proton. For realistic parameters, typically more than one initial proton state will contribute to the rate constant, so eq 2.9 will have to be evaluated.

The above derivation uses the Golden Rule, nonadiabatic version of charge-transfer theory.[19] If the coupling V_{el} becomes sufficiently large, on the order of the temperature, then the adiabatic limit of charge-transfer theory is obtained. In that case, the coefficient $c_{NA} = V_{el}^2/\hbar[\lambda_s k_B T]^{1/2}$ in eq 2.9 is replaced by the coefficient $c_A = \omega_s/2\pi$.[49,52] The frequency ω_s characterizes the rate of the solvent polarization fluctuations and is typically around 10 ps.[43] The activation energy is also somewhat decreased.[49]

III. Construction of the Repulsive Surface

The rate constant formalism presented above assumes a bound initial and a repulsive final proton potential energy surface. The appropriate surfaces are a sum of the gas-phase and electronically solvated surfaces. We refer to a proton potential surface solvated by the electronic polarization of the solvent as a pels (proton electronically solvated) surface. The origin of this electronic solvation is the time scale separation between the (slow) proton and the (fast) electronic degrees of freedom of the solvent (its electronic polarization). The solvent's electronic degrees of freedom instantaneously adjust to the solute configuration. In essence, the pels surface can be viewed as a potential of mean force for the solute's hydrogen-bonded-proton position, in a zero temperature (ground-state) electronic degree of freedom solvent.[43] Of course, the rate constant also depends on the slow (with respect to all the other degrees of freedom) orientational polarization of the solvent, as embodied in the reorganization and free energy terms that contribute to eq 2.9.

For the proton surface when the electron is in its initial state, the effect of electronic solvation can be important numerically. However, it is not critical in the sense that the surface will still be of a double well form and, for the proton initial state, give bound state energy levels. For the electron final state, and when the proton has transferred, the relevant coordinate is the $[R_1O\cdots HNR_2]^{\bullet+}$ hydrogen bond stretch. For cation radicals of this type, the dissociation energy for the hydrogen bond stretch is around 4 kcal/mol.[39] Such energies are typical of hydrogen bond dissociation energies.[37] The binding energy is sufficiently weak that the increasing electronic solvation of the solute as the hydrogen bond stretches is capable of converting the bound surface to a repulsive surface. The enhanced solvation with the bond stretch arises from the increasing charge separation as the hydrogen-bonded cation radical is dissociated. To motivate this point, consider the usual treatment of solvation for obtaining reorganization energies in electron-transfer theory.[45,53] The dependence of the reorganization energy on the separation R_{AD} of two ions of radii a_A and a_D is

$$\lambda_s \sim (\Delta e)^2\left[\frac{1}{2a_D}+\frac{1}{2a_A}-\frac{1}{R_{AD}}\right] \quad (3.1)$$

where Δe is the charge transferred in the reaction. There is an increase in solvation energy of magnitude $(\Delta e)^2(1/d_{AD})$ as the solute is separated from the contact distance d_{AD} to infinity (dissociation for the reaction considered here)

The pels surface can be thought of as arising from the following effective Hamiltonian

$$H_s^{eff} = H_s - \frac{1}{8\pi}\left(1-\frac{1}{\epsilon_\infty}\right)\int d\mathbf{r}\, \mathbf{D}^2 \quad (3.2)$$

where H_s is the gas-phase Hamiltonian of the solute.[54] The solvent properties enter through **D**, the instantaneous electric displacement when the solute is in a given configuration—here characterized by the proton coordinate q—and ϵ_∞ is the solvent's high-frequency dielectric constant. In accord with the solvation being purely electronic, the high-frequency dielectric constant of the solvent appears, as opposed to the static dielectric constant that would be appropriate to equilibrium (Born) solvation. The

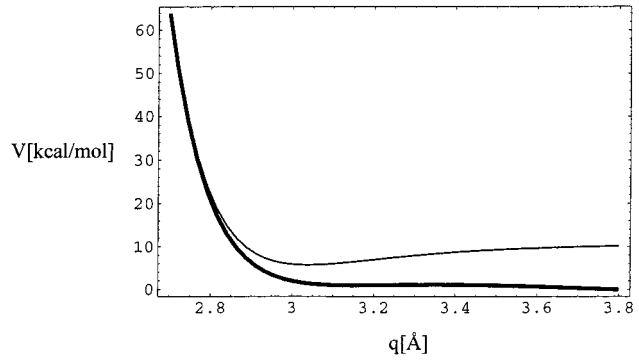

Figure 1. Lippincott−Schroeder gas-phase surface $V_g(q)$ (solid line) and electronically solvated pels surface $V_f^{pels}(q) = V_g(q) + V_f^{els}(q)$ (bold line) as a function of the oxygen−hydrogen distance, q. The electron has transferred, and the coordinate describes the breaking of the O···H hydrogen bond. The pels surface is repulsive. The parameters of the gas-phase surface are given following eq 3.4, those for the electronic solvation following eq 3.3, and those for the fit to the pels surface following eq 3.5.

D field depends parametrically on the solute configuration. The second term of eq 3.2 provides a general expression, within the context of a dielectric formalism, for obtaining the dependence of the electronic solvation on the proton coordinate. The pels surface is obtained by adding this factor to the gas-phase pes in H_s. As a simple model for this solvation, we may treat $R_1O\cdots H^+NR_2$ as a dipole, from the R_1O moiety, and a charge, from the H^+NR_2 moiety. The solvation contribution to eq 3.2 can then be worked out as a function of the O···H distance q. The result for the interaction energy between the dipole of magnitude μ and the charge e (the analog of the $1/R_{AD}$ term in eq 3.1) that gives the excess over the individual solvation parts (the analog of the $1/a_A$ and $1/a_D$ terms in eq 3.1) can be worked out by methods similar to those used for two ions[52] or obtained on the basis of more general methodologies.[55] The result is

$$V_f^{els}(q) \approx \left(1 - \frac{1}{\epsilon_\infty}\right)\frac{\mu e}{q^2} \tag{3.3}$$

Using $e = 1$ and $\mu = 5$ D as representative values, the scale of excess solvation is around 28(7) kcal/mol for a contact distance of 2.5(5) Å.

The gas-phase surface will be based on a Lippincott−Schroeder form (LS):[56]

$$V_g(q,R_{ON}) = be^{-aR_{ON}} + D_e[1 - e^{-n_O(q-d_O)^2/2q}] + CD_e[1 - e^{-n_N(R_{ON}-q-d_N)^2/2(R_{ON}-q)}] \tag{3.4}$$

as it is a reasonable description of, e.g., an OHN hydrogen-bonded system, at least if some if its parameters are adjusted to fit ab initio data.[57] R_{ON} denotes the heavy atom framework separation. The parameters we use are as follows: $b = 2.4 \times 10^{13}$ kcal/mol; $a = 9.8$ Å^{-1}; $D_e = 110$ kcal/mol; $d_O = 0.95$ Å; $d_N = 0.97$ Å; $C = 0.85$; $n_O = 9.18$ Å^{-1}; $n_N = 13.3$ Å^{-1}. With these choices of parameters, the LS surface can be used to represent the stretching and breaking of the hydrogen bond for the final state where the electron and proton have transferred. The surface is plotted in Figure 1. The addition of the electronic solvation component from eq 3.3 (with a cutoff at contact) to the LS surface provides the pels surface, $V_f^{pels}(q) = V_g(q) + V_f^{els}(q)$, shown in Figure 1. The distance 2.5 Å that we use for the contact distance essentially corresponds to the ON distance in the hydrogen-bonded cation radical. The resulting pels surface is repulsive in character. We fit it to an exponential form for convenience in the evaluation of the rate constant values:

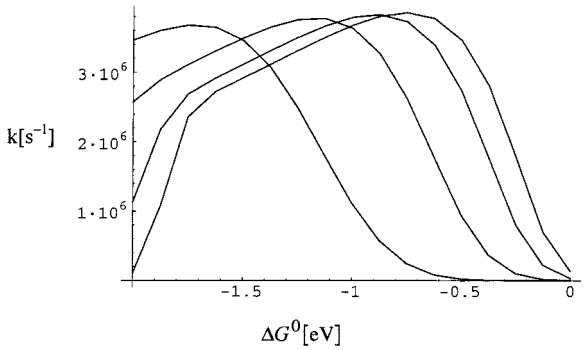

Figure 2. DETPT rate constant k as a function of $\Delta G°$ for $\lambda_s = 0.125$, 0.25, 0.5, and 1.0 eV. As λ_s increases, the curves shift their respective maxima to more negative $\Delta G°$ values. The decay parameter of the repulsive surface is $\kappa = 10$ Å^{-1}.

$$V_f^{pels}(q) = D_r e^{-\kappa q} \tag{3.5}$$

The values $D_r = 1.8$ eV and $\kappa = 10$ Å^{-1} fit the pels surface in Figure 1 quite well.

Clearly, the particulars of the surface in Figure 1 can only be viewed as illustrative. In this regard, studies of pure proton-transfer reactions also rely on the construction of proton surfaces, and such studies could provide alternatives to the methods used here.[58−69] For example, in a previous calculation, we used molecular dynamics to obtain a pels surface[43] for studying a proton-transfer rate constant. This scheme proceeds by using inducible dipoles on each solvent molecule. For each position of the hydrogen-bonded proton, the electronic solvation energy is obtained by solving for the induced dipoles, parametric on the solvent's and solute's nuclear configuration. An average over a representative equilibrium sample of nuclear solvent configurations is taken, for a fixed proton position. This procedure is repeated for a succession of proton positions to map out an averaged (over the solvent nuclear configurations) pels surface. The result is quite similar to the dielectric evaluation carried out above.

IV. Evaluation of the DETPT Rate Constant

The expression for the rate constant given in eq 2.9 is readily evaluated. While the bound state eigenfunctions and eigenvalues should be those of the left localized states in the double well initial proton pes, for simplicity we have used an oscillator approximation for these quantities. Only for states close to the double well barrier could this cause a significant error. The Boltzmann factors for these states renders their contribution to the sum in eq 2.9 sufficiently small that the changes to the rate constant from a more careful treatment are quite small. The rates will be slightly underestimated by our procedure, as the softer surface would produce somewhat more barrier penetration of the proton initial state probability than is obtained for a harmonic approximation, and the energy levels would be somewhat lower.

"Marcus" plots—the rate constant as a function of $\Delta G°$—are presented in Figures 2 and 3 for several values of λ_s, the reorganization energy, and for two values of κ, the decay constant of the repulsive proton surface. We have used $V_{el} = 1$ cm^{-1} throughout as an electronic coupling matrix element value. The striking feature of these results is that the magnitude of the maximum rates are all quite close to each other, though, naturally, the maxima occur at differing values of $\Delta G°$. The similar rate maxima come about because the continuum of final

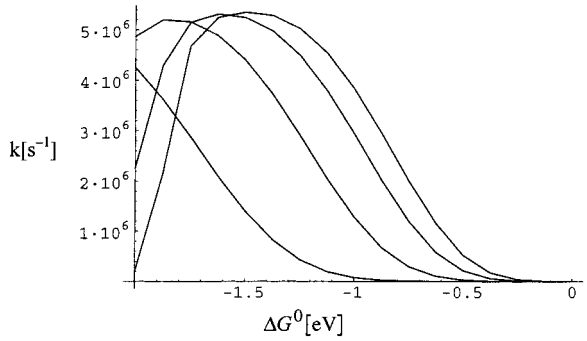

Figure 3. DETPT rate constant k as a function of $\Delta G°$ for $\lambda_s = 0.125$, 0.25, 0.5, and 1.0 eV. As λ_s increases, the curves shift their respective maxima to more negative $\Delta G°$ values. The decay parameter of the repulsive surface is $\kappa = 5$ Å^{-1}.

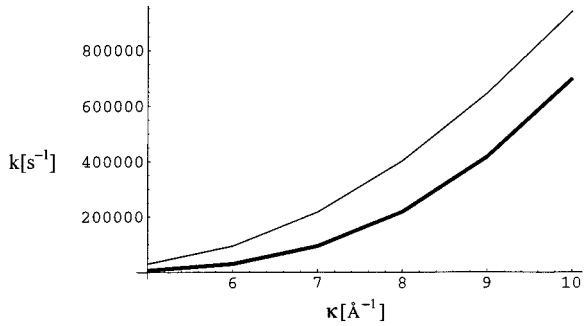

Figure 4. DEPT rate constant k as a function of κ: (bold line) $\lambda_s = 0.125$ eV and $\Delta G° = -0.125$ eV; (solid line) $\lambda_s = 0.5$ eV and $\Delta G° = -0.5$ eV.

proton states provides many opportunities for the quantum transition. This is in marked contrast to ETPT where both initial and final electron/proton states are bound, and the rate constant values depend quite sensitively on the number and energies of the final bound states.[23] Another view of the rate can be obtained by plotting it as a function of κ for fixed values of λ_s and $\Delta G°$. In Figure 4 we do so for κ values spanning 5−10 Å^{-1}, where it is seen that the dependence is dramatic.

The qualitative dependence of k on the free energy of the reaction is easy to understand. As $\Delta G°$ decreases and, in terms of this criterion, becomes exothermic, $\Delta G° < 0$, the (positive) reorganization energy is increasingly canceled. This tends to increase the rate constant. Further increase in exothermicity will then decrease the rate constant. As evident in Figures 2 and 3, increasing λ_s will shift the maximum in the corresponding Marcus plot to greater exothermicity. The complicating factors are the presence of the energy levels ϵ_{1n} and the final state surface $V_2(q)$ in the activation energy, and the equilibrium-weighted proton probabilities. The rate maximum, and the slower decrease in rate with more negative $\Delta G°$ values past the rate maximum, is similar to what is found for ET rates based on coupling the electron to two nuclear modes, one treated classically (the solvent) and the other quantum mechanically (a bond displaced in the ET reaction).[4]

With regard to the effect of the final state surface, the greatest sensitivity is to κ, the decay parameter of the repulsive potential. Figures 2 and 3 show that decreasing κ to 5 Å^{-1} leads to rate maxima for the Marcus plots at perhaps unrealistically large (negative) $\Delta G°$ values. This important dependence of k on κ can be analyzed by reformulating the expression for the rate constant in eq 2.1. Expressing the energy conservation δ function as a Fourier time integral, noting the independence of the solvent and proton modes, and representing the solvent part in terms of a trace over the solvent degrees of freedom lets us write eq 2.1 as

$$k = \frac{V_{el}^2}{\hbar}\sum_{n'}\sum_{n}\int\frac{dt}{\hbar} \rho_{1n'}|\langle\chi_{2n}|\chi_{1n'}\rangle|^2\, e^{-i(\epsilon_{1n'}-\epsilon_{2n})t/\hbar} Tr P_1 e^{iH_2^s t/\hbar} e^{-iH_1^s t/\hbar} \quad (4.1)$$

Taking the classical limit of the solvent contribution, with coordinates that we shall denote collectively as x,

$$Tr P_1 e^{iH_2^s t/\hbar} e^{-iH_1^s t/\hbar} \xrightarrow{classical} \int dx\, P_1(x)\, e^{i(V_2(x)-V_1(x))t/\hbar} \quad (4.2)$$

and expressing the proton Franck−Condon factor in terms of the density matrices as defined in eq 2.6, provides the expression

$$k = \frac{V_{el}^2}{\hbar}\int_{-\infty}^{+\infty}\frac{dt}{\hbar}\int dq\int dq'\,\rho_1(q,q'|\beta - it)\,\rho_2(q,q'|it)\int dx\, P_1(x)\, e^{i(V_2(x)-V_1(x))t/\hbar} \quad (4.3)$$

Now using the classical approximation to ρ_2 given in eq 2.8 and reexpressing ρ_1 in terms of Franck−Condon factors then yield

$$k = \frac{V_{el}^2}{\hbar}\sum_{n'=0}\rho_{1n'}\int dq\,|\chi_{1n'}(q)|^2\int_{-\infty}^{+\infty}\frac{dt}{\hbar}\int dx\, P_1(x) \exp[i(V_2(x) - V_1(x) - (\epsilon_{1n'} - V_2(q))t/\hbar] \quad (4.4)$$

The final step is to carry out the time integral to obtain

$$k = \frac{2\pi V_{el}^2}{\hbar}\sum_{n'=0}\rho_{1n'}\int dq\,|\chi_{1n'}(q)|^2\int dx\, P_1(x)\,\delta(V_2(x) - V_1(x) - (\epsilon_{1n'} - V_2(q))) = \frac{2\pi V_{el}^2}{\hbar}\sum_{n'=0}\rho_{1n'}\int dq\,|\chi_{1n'}(q)|^2\, P_{1n'}(q)\, J(q) \quad (4.5)$$

where in the factor $P_{1n'}(q)$, q is the set of values that satisfy the δ function energy conservation condition in eq 4.5 for a particular proton initial energy $\epsilon_{1n'}$ and $J(q)$ is the Jacobian transforming the energy δ function to the coordinate one to carry out the x integration. The formulation in eq 4.5 shows that the rate constant can be viewed as arising in part from a set of activation energy factors, $P_{1n'}(q)$, evaluated at a set of q values that is determined by the line of intersection of the initial and final state energies in a $q-x$ two-dimensional space. If the transition were completely classical, that is, if we also treated the proton initial state as a classical degree of freedom, then the activation energy contribution to the rate constant would be determined by the minimum energy point along the line of intersection in the two-dimensional $q-x$ space.[70] In the present case, there is a range of q values that will contribute to the effective activation energy. The range of contributing q values is determined by the overlaps of the equilibrium-weighted proton probability factors for each level and the $P_{1n'}(q)$ activation energy factors. This viewpoint shows that increasing the κ value to give a more repulsive surface serves to increase $P_{1n'}(q)$ for a given value of q. In effect, the activation energy is reduced and this corresponds to an increase of the exothermicity toward the activationless point. Thus, as in more conventional charge-transfer reactions, the rate constant is again most sensitive to changes in the reaction exothermicity.

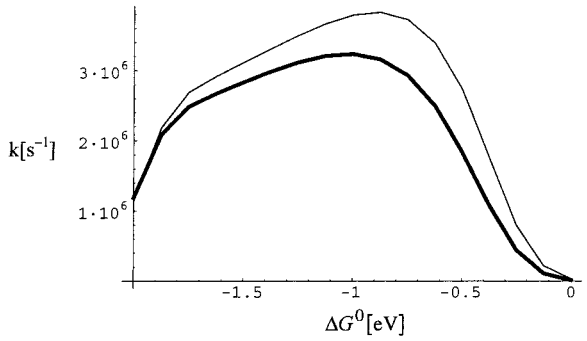

Figure 5. DETPT rate constant k for deuterium (bold line) versus hydrogen (solid line). Here, $\lambda_s = 0.25$ eV and $\kappa = 10$ Å^{-1}. The isotope effect is modest, with the hydrogen/deuterium rate ratio no more than a factor of 2.

It is of interest to replace the proton with a deuteron. That will mainly influence the states in the initial proton surface, because this motion corresponds to the proton/deuteron stretch. For the final state surface, it is the heavy atom framework that is moving and there is only a negligible reduced mass effect. A Marcus plot comparing proton and deuteron rate constants is given in Figure 5. The proton/deuteron rate ratio is no more than a factor of 2. The deuteron rate constant should decrease relative to the proton rate constant, because the deuteron probability densities are considerably narrower than those for the proton. However, the lower energies that the deuteron states occupy in the initial proton well with their associated larger thermal probabilities serve to partly compensate for their narrower wave functions. Thus, the predicted isotope effect is relatively modest.

V. Concluding Remarks

In this article we extended the theory of concerted ETPT to DETPT, dissociative ETPT, where the final proton surface is a repulsive surface. The main ingredients that lead to the rate expression given in eq 2.9 are the repulsive nature of the final state proton surface and a classical treatment of the density matrix that describes this surface. The repulsive surface was constructed by electronically solvating the surface for breaking the hydrogen bond as the cation radical dissociates. Use was made of the separation between the fast electronic solvent polarization and the slow, relative to this polarization, proton motion to define the pels surface as a potential of mean force. In contrast, the energetic interaction between the solvent and the transferring charges is evaluated parametrically on the solvent configurations, because the solvent's orientational polarization is slow compared with the proton and electron time scales, as in electron-transfer theory. Thus, both the fast electronic polarization and the slow orientational polarization effects enter the ETPT rate expression. These features lead to an activation energy expression that is specific to each initial proton state, because the proton is treated quantum mechanically. For the proton final state, its continuum of energies on the repulsive surface leads to an integration over the final state coordinate or, equivalently, final state energies. This "averaging" over final state energies leads to rate constant values that can be large for suitable values of the solvent reorganization energy and the reaction exothermicity.

The use of a classical approximation to the final proton state density matrix (eq 2.8) will break down for sufficiently steep repulsive surfaces. An estimate of the validity of the classical approximation is the condition that $\Lambda\kappa < 1$, where Λ is the thermal deBroglie wavelength and κ is the repulsive surface decay constant. For a reduced mass of 100 amu, as an estimate of the final proton state fragment mass, $\Lambda\kappa \sim 1$ when $\kappa = 10$ Å^{-1}. Thus, for such a steeply repulsive pes the classical approximation becomes questionable. However, the alternative of using semiclassical approximations to the Franck−Condon factors between the bound initial and unbound final proton surfaces that enter eq 2.3 would introduce uncertainties that are difficult to quantitate. It is also the case that the validity of the classical approximation depends on the characteristics of the bound state proton surface. To this end, we are examining semiclassical approximations to the Franck−Condon factors in eq 2.3 that can be compared with exact quantum mechanical results to assess their validity.[71]

We explored the dependence of the rate on the parameters and found that the shape of the plots of k versus $\Delta G°$ are reminiscent of those found for a Marcus one classical (solvent) and one quantum (bond) mode ET theory. The rate values depend sensitively on the decay parameter of the repulsive proton surface because, as shown in eq 4.5, the repulsive surface may be viewed as providing a (q-dependent) contribution to the reaction exothermicity. With regard to the magnitude of the rate constant, the choice of $V_{el} = 1$ cm^{-1} produces maximum rates in the 10^6-10^7 ps^{-1} range. In the adiabatic limit, where the rate prefactor is given by $c_A = \omega_s/2\pi$, the rate increases by about 3 orders of magnitude over the nonadiabatic value to around 10^{10} ps^{-1}. Therefore, DETPT can lead to rate constants that are quite large. However, DETPT, at least by the mechanism presented above, will not produce rates in the 10^{12} ps^{-1} range, as has been found for some ET and PT reactions. As we have discussed previously,[22] in contrasting the consecutive reaction pathway, ET/PT, with the concerted pathway, ETPT, the limitation on overall conversion for ET/PT is that of a rate limiting step, while, for ETPT, the longer tunneling path required to quantum mechanically transfer the electron and proton limits the rate constant's magnitude. For DETPT there is the same limitation as for ETPT; nevertheless, the rate constants can be quite large. Thus, DETPT may be a dominant channel for coupled electron and proton transfer.

In the coupled proton electron transfer for the photosystem II oxygen evolving complex (PSII/OEC) that we discussed in the Introduction, rates on the order of 10^6-10^7 s^{-1} are observed.[72] Furthermore, recent experiments have examined the isotope effect on the rate and found a roughly 2-fold rate decrease upon deuteration.[33] Both these observations are consistent with the DETPT rate mechanism proposed here. Unfortunately, in the work of Linschitz and co-workers,[35] the quenching of the proton-transfer complex by C_{60} is a bimolecular process, so we cannot compare our (unimolecular) rate constants with their rate constants. However, they also investigated the isotope effect and found a roughly 2-fold decrease of the quenching rate upon deuteration.

Acknowledgment. The financial support of the National Institutes of Health (Grant GM 47274) is gratefully acknowledged.

References and Notes

(1) Okamura, M. Y.; Feher, G. *Annu. Rev. Biochem.* **1992**, *61*, 861.
(2) Malmström, B. G. *Acc. Chem. Res.* **1993**, *26*, 332.
(3) Ferguson-Miller, S.; Babcock, G. T. *Chem. Rev.* **1996**, *96*, 2889.
(4) Hoganson, C. W.; Babcock, G. T. *Science* **1997**, *277*, 1952.
(5) Birge, R. R. *Annu. Rev. Phys. Chem.* **1990**, *41*, 683.
(6) Durr, H.; Bouas-Laurent, H. *Photochromism: Molecules and Systems*; Studies in Organic Chemistry 40; Elsevier: Amsterdam, 1990.
(7) Scherl, M.; Haarer, D.; Fischer, J.; DeCian, A.; Lehn, J.-M.; Eichen, Y. *J. Phys. Chem.* **1996**, *100*, 16175.

(8) Roecker, L.; Meyer, T. J. *J. Am. Chem. Soc.* **1987**, *109*, 746.
(9) Thorp, H. H. *Inorg. Chem.* **1991**, *3*, 171.
(10) Shafirovich, V. Y.; Courtney, S. H.; Ya, N.; Geacintov, N. E. *J. Am. Chem. Soc.* **1995**, *117*, 4920.
(11) Binstead, R. A.; McGuire, M. E.; Dovletoglou, A.; Seok, W. K.; Roecker, L. E.; Meyer, T. J. *J. Am. Chem. Soc.* **1992**, *114*, 173.
(12) Turro, C.; Chang, C. K.; Leroi, G. E.; Cukier, R. I.; Nocera, D. G. *J. Am. Chem. Soc.* **1992**, *114*, 4013.
(13) Kirby, J. P.; Dantzig, N. A. v.; Chang, C. K.; Nocera, D. G. *Tetrahedron Lett.* **1995**, *36*, 3477.
(14) Roberts, J. A.; Kirby, J. P.; Nocera, D. G. *J. Am. Chem. Soc.* **1995**, *117*, 8051.
(15) Roberts, J. A.; Kirby, J. P.; Wall, S. T.; Nocera, D. G. *Inorg. Chim. Acta* **1997**, *263*, 395.
(16) Deng, Y.; Roberts, J. A.; Peng, S. M.; Chang, C. K.; Nocera, D. G. *Angew. Chem., Int. Ed. Engl.* **1997**, *36*, 2124.
(17) Kirby, J. P.; Roberts, J. A.; Nocera, D. G. *J. Am. Chem. Soc.* **1997**, *119*, 9230.
(18) Krishtalik, L. I. *Adv. Electrochem. Electrochem. Eng.* **1970**, *7*, 283.
(19) Levich, V. G. In *Physical Chemistry-An Advanced Treatise*; Henderson, H., Yost, W., Eds.; Academic: New York, 1970; Vol. 9B, p 985.
(20) Cukier, R. I. *J. Phys. Chem.* **1994**, *98*, 2377.
(21) Zhao, X. G.; Cukier, R. I. *J. Phys. Chem.* **1995**, *99*, 945.
(22) Cukier, R. I. *J. Phys. Chem.* **1995**, *99*, 16101.
(23) Cukier, R. I. *J. Phys. Chem.* **1996**, *100*, 15428.
(24) Cukier, R.; Nocera, D. *Annu. Rev. Phys. Chem.* **1998**, *49*, 337.
(25) Benderskii, V. A.; Grebenshchikov, S. Y. *J. Electroanal. Chem.* **1994**, *375*, 29.
(26) Fang, J.-Y.; Hammes-Schiffer, S. *J. Chem. Phys.* **1997**, *106*, 8442.
(27) Fang, J.-Y.; Hammes-Schiffer, S. *J. Chem. Phys.* **1997**, *107*, 5727.
(28) Fang, J.-Y.; Hammes-Schiffer, S. *J. Chem. Phys.* **1997**, *107*, 8933.
(29) Meyer, B.; Scholddr, E.; Dekker, J. P.; Witt, H. T. *Biochim. Biophys. Acta* **1989**, *974*, 36.
(30) Tommos, C.; Tang, X.-S.; Warncke, K.; Hoganson, C. W.; Styring, S.; McCracken, J.; Diner, B. A.; Babcock, G. T. *J. Am. Chem. Soc.* **1995**, *117*, 10325.
(31) Chu, H.-A.; Nguyen, A. P.; Debus, R. *Biochemistry* **1995**, *34*, 5839.
(32) Tommos, C.; Babcock, G. T. *Acc. Chem. Res.* **1998**, *31*, 18.
(33) Diner, B. A.; Force, D. A.; Randall, D. W.; Britt, R. D. *Biochemistry*, in press.
(34) Biczok, L.; Linschitz, H. *J. Phys. Chem.* **1995**, *99*, 1843.
(35) Biczok, L.; Gupta, N.; Linschitz, H. *J. Am. Chem. Soc.* **1997**, *119*, 12601.
(36) Brede, O.; Orthner, H.; Zubarev, V.; Hermann, R. *J. Phys. Chem.* **1996**, *100*, 7097.
(37) Zeeger-Huyskens, T.; Huyskens, P. Molecular Interactions. In *Proton transfer and ion transfer complexes*; Ratajczak, H., Orville-Thomas, W. J., Eds.; Wiley: New York, 1980; Vol. 2, p 1.
(38) Hobza, P.; Burel, R.; Spirko, V.; Dopfer, O.; Müller-Dethlefs, K.; Schlag, E. W. *J. Chem. Phys.* **1994**, *101*, 990.
(39) Haines, S. R.; Geppart, W. D.; Chapman, D. M.; Watkins, M. J.; Dessent, C. E. H.; Cockett, M. C. R.; Müller-Dethlefs, K. *J. Chem. Phys.* **1998**, *109*, 9244.
(40) Re, S.; Osamura, Y. *J. Phys. Chem. A* **1998**, *102*, 3798.
(41) Sodupe, M.; Oliva, A.; Bertran, J. *J. Phys. Chem. A* **1997**, *101*, 9142.
(42) Yi, M.; Scheiner, S. *Chem. Phys. Letts.* **1996**, *262*, 567.
(43) Cukier, R. I.; Zhu, J. *J. Phys. Chem.* **1997**, *101*, 7180.
(44) Marcus, R. A. *J. Chem. Phys.* **1956**, *24*, 979.
(45) Marcus, R. A. *J. Chem. Phys.* **1956**, *24*, 966.
(46) Savéant, J.-M. *Acc. Chem. Res.* **1993**, *26*, 455.
(47) Zhu, J.; Spirina, O. B.; Cukier, R. I. *J. Chem. Phys.* **1994**, *100*, 8109.
(48) German, E. D.; Kuznetsov, A. M. *J. Phys. Chem.* **1994**, *98*, 6120.
(49) Ulstrup, J. *Charge Transfer Processes in Condensed Media*; Springer: Berlin, 1979.
(50) Kestner, N. R.; Jortner, J.; Logan, J. *J. Phys. Chem.* **1974**, *78*, 2148.
(51) Cukier, R. I.; Morillo, M. *J. Chem. Phys.* **1989**, *91*, 857.
(52) Marcus, R. A. *Annu. Rev. Phys. Chem.* **1964**, *15*, 155.
(53) Marcus, R. A.; Sutin, N. *Biochim. Biophys. Acta* **1985**, *811*, 265.
(54) Zhu, J. J.; Cukier, R. I. *J. Chem. Phys.* **1995**, *102*, 8398.
(55) Phillies, G. *J. Chem. Phys.* **1974**, *60*, 2721.
(56) Lippincott, E. R.; Schroeder, R. *J. Chem. Phys.* **1955**, *23*, 1099.
(57) Vener, M. V. *Chem. Phys. Lett.* **1995**, *244*, 89.
(58) Warshel, A. *J. Phys. Chem.* **1982**, *86*, 2218.
(59) Laria, D.; Ciccotti, G.; Ferrario, M.; Kapral, R. *J. Chem. Phys.* **1992**, *97*, 378.
(60) Laria, D.; Kapral, R.; Estrin, D.; Ciccotti, G. *J. Chem. Phys.* **1996**, *104*, 6560.
(61) Lobaugh, J.; Voth, G. A. *Chem. Phys. Lett.* **1992**, *198*, 311.
(62) Lobaugh, J.; Voth, G. A. *J. Chem. Phys.* **1994**, *100*, 3039.
(63) Bala, P.; Lesyng, B.; McCammon, J. A. *Chem. Phys.* **1994**, *180*, 271.
(64) Hammes-Schiffer, S.; Tully, J. C. *J. Chem. Phys.* **1994**, *101*, 4657.
(65) Mavri, J.; Berendsen, H. J. C.; Gunsteren, W. F. v. *J. Phys. Chem.* **1993**, *97*, 13469.
(66) Mavri, J.; Berendsen, H. J. C. *J. Phys. Chem.* **1995**, *99*, 12711.
(67) Staib, A.; Borgis, D.; Hynes, J. T. *J. Chem. Phys.* **1995**, *102*, 2487.
(68) Borgis, D.; Hynes, J. T. *J. Phys. Chem.* **1996**, *100*, 1118.
(69) Ando, K.; Hynes, J. T. *J. Phys. Chem. B* **1997**, *101*, 10464.
(70) Christov, S. G. *Philos. Mag. B* **1985**, *52*, 71.
(71) Cukier, R. I. Work in progress.
(72) Babcock, G. T.; Barry, B. A.; Debus, R. J.; Hoganson, C. W.; Atamian, M.; McIntosh, L.; Sithole, I.; Yocum, C. F. *Biochemistry* **1989**, *28*, 9557.